Supplement of Biogeosciences, 23, 2389–2412, 2026
https://doi.org/10.5194/bg-23-2389-2026-supplement

Biogeosciences Open Access EGU

Supplement of

River flooding reshapes sediments, contaminants and benthic microbial communities in a Mediterranean coastal system

Claudio Pellegrini et al.

Correspondence to: Irene Sammartino (irene.sammartino@cnr.it)

DATA AND METHODS

Meteorological and oceanographical datasets

Meteorological data were obtained from the MOLOCH model (Davolio et al., 2017), a non-hydrostatic, convection-permitting numerical weather prediction system with 1.25 km horizontal resolution, providing 48-hour forecasts at hourly intervals.

Oceanographic data were derived from the Adriac operational forecasting system implementing the Coupled-Ocean-Atmosphere-Wave-Sediment Transport (COAWST) model (Regional Ocean Modelling System, ROMS + Simulating Waves Nearshore, SWAN) at 1 km horizontal resolution with 72-hour forecasts (Warner et al., 2010; Bressan et al., 2017). Model outputs are publicly accessible at https://dati-simc.arpae.it/opendata/adriac/.

Complementary observational data include measurements from the TeleSenigallia marine weather station, equipped with an upward-looking Acoustic Doppler Current Profiler (ADCP; Ravaioli et al., 2016) and the ANCONA wave buoy of the Italian National Wave Buoy Network (ISPRA - Italian Institute for Environmental Protection and Research).

Sedimentological analyses on organic and inorganic particles

Sediment samples with notable texture changes were stabilized with Spurr resin after pore water removal using acetone, following Schimmelmann et al. (2015). Samples were then ion-milled according to Schieber (2013) to expose smooth surfaces suitable for Scanning Electron Microscopy (SEM) analysis. SEM imaging was performed using a FEI Quanta 400 FEG (Field Emission Gun) scanning electron microscope in low vacuum mode, without applying conductive coating to preserve natural sediment fabric. Compositional analyses were carried out by Energy Dispersive X-ray Spectroscopy (EDS).

Granulometric analyses were conducted on aliquots dried at 50°C for 24 hours. Grain-size distributions were obtained using a Malvern Panalytical Mastersizer 3000 laser diffraction analyzer (range 0.01–3500 μm), after sample dispersion and ultrasonication. Laser-scattering spectra were processed with the Multiple Sample Statistics function in the GRADISTAT Microsoft Excel worksheet (Blott and Pye, 2001). Grain-size classes were reported according to the Wentworth scale (Wentworth, 1922).

Stable carbon isotope analyses ($\delta^{13}C$) of sedimentary organic carbon were performed on bulk sediment samples acidified to remove inorganic carbon, using a Fisons NA2000 Elemental Analyzer (EA) coupled with a Finnigan Delta Plus Isotope Ratio Mass Spectrometry (IRMS), following Tesi et al. (2007). Analytical precision was better than ±0.1‰ based on standards IAEA-CH-7 (International Atomic Energy Agency) and in-house replicates. A compilation of $\delta^{13}C$ values from terrigenous sources along the Adriatic coast was used to define source end-members, incorporating data from Po River suspended sediments (2011 flood), Apennine river-bed sediments (2005), and Po River flood deposits (2000–2009), averaging -26.46 ± 0.44‰ (Tesi et al., 2013; Pellegrini et al., 2021, 2024). These data supported the apportionment of organic carbon sources in the study area (Tesi et al., 2013; Pellegrini et al., 2021). Data are summarized in table S1.

X-Ray Fluorescence (XRF)

Bulk sediment powders were prepared by grinding samples with an agate swing mill and pressing into 40 mm diameter tablets. Wavelength Dispersive (WD) XRF analyses were conducted at the University of Bologna using a Malvern Panalytical Axios spectrometer equipped with a Rh anode X-ray tube. Matrix corrections followed protocols outlined by Franzini et al. (1972, 1975) and Leoni and Saitta (1976). Accuracy and precision were verified using Certified Reference Materials (CRMs; Govindaraju, 1989), with uncertainties approximately 2% for Ni and Zn, 6% for Cu, 7% for Cr, and 10% for As and Pb. Data are summarized in table S1.

Polycyclic Aromatic Hydrocarbons (PAHs)

PAHs were extracted from 1 g of dried sediment samples using an ultrasonic-assisted solvent extraction, with a 1:1 (v/v) dichloromethane:methanol mixture in three successive cycles of 15 minutes each. Extracts were then concentrated under rotary evaporation at 27°C with a gentle nitrogen flow and reconstituted in 0.4 mL of acetonitrile. PAHs were analyzed using a Thermo Scientific UltiMate 3000 Ultra High Performance Liquid Chromatograph (UHPLC), equipped with diode array and fluorescence detectors, following the method detailed in Frapiccini et al. (2024).

Method validation conformed to ICH Q2B guidelines of the European Medicines Agency. Recoveries were verified with IAEA CRMs. According to sediment quality guideline criteria, PAH contamination ranged from low to moderate levels (Yunker et al., 2002). Data are summarized in tables S1, S2 and S3 and in figure S1.

Poly- and Perfluorinated Alkyl Substances (PFASs)

Approximately 10 g of wet sediment samples were homogenized and mixed with diatomaceous earth, anhydrous sodium sulfate, and activated Cu to remove humidity and elemental S, then spiked with a known amount of D and ^{13}C isotope-labeled solution. An Accelerated Solvent Extraction (ASE) at 100 bar and 100°C was conducted, using methanol as extraction solvent, with three static 5-minute cycles per sample. Extracts were collected together, evaporated at 30°C under a gentle nitrogen stream to 10 mL, and then diluted with 25 mL of deionized water. Clean-up was performed by Solid Phase Extraction (SPE) using Waters Oasis HLB (Hydrophilic-Lipophilic Balance) cartridges (500 mg, 6 mL, 60 μm).

Instrumental analysis was performed with an Agilent Technologies 1100 Series HPLC coupled with a MDS SCIEX API 4000™ triple quadrupole tandem Mass Spectrometer (MS/MS), equipped with an ElectroSpray Ionization (ESI) Turbo V™ source, operated in negative polarity. Data acquisition was obtained in Multiple Reaction Monitoring (MRM) mode with a 50 ms dwell time/transition. The quality control of the entire analytical procedure, in terms of repeatability, trueness, and percentage of recovery, was performed on five replicates of a fortified real environmental matrix. Sediments collected at a depth of 10 m in the Venice Lagoon, dating back to the Pleistocene and therefore considered free of modern contaminants, were used (Pizzini et al., 2024). Data are summarized in tables S1 and S4.

Microbial communities

DNA was extracted from the top 0–1 cm of sediment using standard protocols. The V4–V5 hypervariable regions of the 16S rRNA gene were amplified using primers 518F and 926R (Parada et al., 2016). Libraries were prepared according to the Nextera protocol and sequenced on an Illumina NextSeq 2000 platform (2 × 300 bp paired-end reads).

Raw sequence data were processed using Cutadapt (Martin, 2011) for adapter trimming, followed by DADA2 (Callahan et al., 2016) for quality filtering, chimera removal, and Amplicon Sequence Variant (ASV) inference. Quality thresholds included maximum expected errors >2 for forward and reverse reads. Taxonomic classification was performed using a naive Bayesian classifier trained on the SILVA v138 database (Quast et al., 2013). Chloroplast and eukaryotic sequences were filtered out.

Alpha (ASV richness) and beta diversity metrics were calculated using the *vegan* and *phyloseq* packages in R (McMurdie and Holmes, 2013; Oksanen et al., 2025). Beta diversity was assessed by Non-metric Multidimensional Scaling (nMDS), and PERMANOVA tested for significant community differences among transects. Linear discriminant analysis Effect Size (LEfSe) was performed to identify taxa characterizing the coastal, prodelta, and offshore groups (Segata et al., 2011). Freshwater-associated taxa identification followed Massaccesi et al. (2025). Raw sequence data are publicly available at Sequence Read Archive (SRA) of the National Center for Biotechnology Information (NCBI; accession PRJNA1280684). Data are summarized in table S1, and figures S2 and S3.

		Grain size (%)			X-Ray Fluorescence (XRF) (mg g^{-1})						Poly- and Perfluorinated alkyl substances (PFASs) (ng g^{-1})		Organic Matter (OM)			Microbial communities								Polycyclic Aromatic Hydrocarbons (PAHs)
	Sampling site	SAND	SILT	CLAY	As	Cr	Cu	Ni	Pb	Zn	6:2 FTS	8:2 FTS	TN (%)	TOC (%)	δ13C (‰)	Thermoanaerobaculaceae	Desulfobulbaceae	Woeseiaceae	Unknown family	Cyclobacteriaceae	Not assigned	Not assigned	Not assigned	Pirellulaceae	Flavobacteriaceae	Σ16PAHs
2022 flood sediments	RRC22-01	7.1	87.6	5.3	9	55	20	33	17	47	10.45	0	0.02	0.11	-22.79	9.36	3.41	10.11	4.52	2.54	4.84	8.69	2.37	7.57	1.56	51.97
	RRC22-02	61.3	37.6	1	9	83	21	36	15	49	NA	NA	0.03	0.13	-23.28	10.94	4.53	7.54	3.96	2.80	3.44	10.90	2.71	7.14	1.24	NA
	RRC22-03	38.5	59.8	1.7	11	106	39	70	25	100	58.60	0.35	0.08	0.63	-24.78	5.60	4.81	8.24	7.39	3.20	2.14	3.37	2.44	5.60	3.47	47.03
	RRC22-04	33.9	63.5	2.6	10	92	30	49	17	61	65.34	0.25	0.06	0.43	-23.98	8.76	3.72	6.11	5.68	1.91	2.63	3.50	1.91	9.10	2.04	49.56
	RRC22-05	52.7	46.5	0.9	15	100	29	58	22	85	NA	NA	0.04	0.28	-24.33	8.35	7.28	7.13	4.21	2.93	2.03	5.22	2.02	6.80	1.58	NA
	RRC22-06	88	11.7	0.3	8	60	19	26	13	32	85.70	0.39	0.02	0.09	-22.93	9.81	3.15	11.02	5.61	2.24	5.05	8.04	2.19	8.16	1.34	17.82
	RRC22-07	NA	NA	NA	8	42	23	27	15	31	86.10	0.44	0.04	0.09	-22.8	8.41	3.25	10.36	4.68	2.31	5.32	6.97	2.21	6.51	2.00	39.42
	RRC22-08	52.3	46.5	1.2	10	99	26	40	17	56	NA	NA	0.04	0.24	-24.62	9.52	6.01	8.18	4.97	2.49	3.60	6.91	2.38	5.75	1.90	NA
	RRC22-09	NA	NA	NA	11	92	28	50	21	70	38.60	0.21	0.06	0.35	-24.28	7.13	3.95	9.12	7.49	3.19	3.18	4.08	2.47	7.53	2.56	63.55
	RRC22-10	15.4	79.0	3.5	9	102	35	57	24	81	0.88	0	0.11	0.83	-25.27	4.51	4.40	6.60	6.04	3.69	1.15	2.89	2.77	4.11	3.49	69.40
	RRC22-11	47	51.1	1.9	12	86	29	52	20	73	NA	NA	0.05	0.34	-23.79	7.68	5.14	6.75	5.02	2.99	2.21	5.10	2.28	6.08	2.17	NA
	RRC22-12	88.4	11.4	0.3	8	43	17	26	13	28	0.79	0	0.02	0.11	-23.07	11.21	3.07	10.72	6.25	2.45	4.00	9.82	2.53	7.47	1.24	25.63
	RRC22-13	95.2	4.8	0.1	7	73	18	20	14	21	45.18	0.25	0.01	0.08	-23.12	10.31	1.81	11.27	3.94	1.52	5.38	6.51	2.76	6.73	2.27	24.89
	RRC22-14	62.0	37.0	0.9	10	65	22	31	12	57	NA	NA	0.04	0.23	-24.4	8.53	4.54	6.71	5.64	2.57	3.79	8.80	1.85	7.07	1.75	NA
	RRC22-15	7.6	86.7	5.2	12	95	40	69	21	89	0.65	0	0.16	1.23	-26.07	2.66	3.55	3.95	4.58	2.57	0.46	1.83	2.41	2.62	4.97	141
	RRC22-16	10.8	87.2	2.0	14	103	27	58	24	83	NA	NA	0.12	0.75	-23.77	7.01	4.45	8.12	5.80	3.05	1.92	4.57	1.57	6.93	1.96	NA
	RRC22-17	26	70.6	3.5	11	92	35	55	19	72	0.34	0	0.11	0.87	-25.8	3.86	3.11	3.55	5.04	2.97	0.71	2.80	2.74	2.90	4.59	30.90
	RRC22-18	70.3	29.0	0.6	10	74	16	30	11	33	NA	NA	0.04	0.17	-23.51	9.57	5.24	7.42	4.60	2.65	3.11	7.16	2.12	7.00	1.53	NA
	RRC22-19	87.1	12.8	0.2	6	47	13	22	14	24	0.41	0	0.03	0.13	-23.23	9.22	3.38	8.98	4.79	1.87	4.95	7.42	1.70	8.35	1.35	30.49
	RRC22-20	92.5	7.3	0.2	NA	NA	NA	NA	NA	NA	0.50	0	0.02	0.12	-23.03	9.41	2.32	12.00	4.06	0.96	3.07	6.03	2.42	7.93	2.54	23.69
	RRC22-21	49.7	47.9	2.3	10	55	19	32	12	38	NA	NA	0.06	0.41	-24.85	7.62	4.91	7.36	4.93	2.73	2.09	5.74	2.03	5.58	2.74	NA
	RRC22-22	7.1	87.6	5.3	12	92	36	64	19	86	0.20	0	0.14	1.09	-25.79	3.36	3.19	4.01	5.53	2.76	0.87	2.87	2.37	2.96	4.37	34.01
	RRC22-23	7.1	89.4	3.4	NA	NA	NA	NA	NA	NA	NA	NA	0.1	0.67	-24.21	6.51	5.29	8.60	5.61	4.05	1.56	4.71	2.23	7.55	1.96	NA
	RRC22-24	68.3	30.2	1.5	NA	NA	NA	NA	NA	NA	0	0	0.02	0.13	-23.53	8.88	2.47	9.08	3.98	2.31	3.52	6.80	2.33	7.66	2.13	42.99
	RRC22-25	18.5	77.0	4.5	NA	NA	NA	NA	NA	NA	NA	NA	0.1	0.68	-24.88	3.89	3.37	5.38	5.54	2.51	1.13	2.56	2.39	3.84	3.68	NA
	RRC22-26	5.6	89.6	4.7	NA	NA	NA	NA	NA	NA	0	0	0.02	0.10	-23.49	2.61	2.86	4.79	4.84	2.83	0.79	1.81	2.57	2.51	3.35	14.61
	RRC22-27	15.1	82.3	2.7	NA	NA	NA	NA	NA	NA	NA	NA	0.1	0.70	-23.67	6.82	4.85	7.93	4.89	3.50	1.99	4.53	2.18	8.16	1.89	NA
	RRC22-28	9.3	87.0	3.7	NA	NA	NA	NA	NA	NA	NA	NA	0.13	0.89	-24.5	NA	NA	NA	NA	NA	NA	NA	NA	NA	NA	NA
	RRC22-29	39.2	57.8	3.0	NA	NA	NA	NA	NA	NA	0	0	0.07	0.42	-24.35	7.53	3.28	7.43	5.52	3.46	3.97	7.44	1.83	5.86	2.69	24.76
	RRC22-30	40.2	57.4	2.4	NA	NA	NA	NA	NA	NA	NA	NA	0.08	0.36	-23.89	7.14	3.54	8.01	6.24	3.37	2.53	5.62	2.59	5.27	3.12	NA
	RRC22-31	76.6	22.8	0.6	NA	NA	NA	NA	NA	NA	0	0	0.02	0.13	-23.4	8.64	2.59	8.29	5.42	2.84	2.20	6.71	2.72	5.94	2.78	14.37
Sediments underlying the flood event	RRC22-01	87.6	12.4	0.2	8	61	25	33	17	48	NA	NA	0.02	0.09	-22.44	NA	NA	NA	NA	NA	NA	NA	NA	NA	NA	NA
	RRC22-02	84.0	16.0	0.2	10	75	18	31	14	41	NA	NA	0.02	0.10	-22.85	NA	NA	NA	NA	NA	NA	NA	NA	NA	NA	NA
	RRC22-03	50.2	49.8	0.9	10	80	24	44	18	60	0.46	NA	0.03	0.16	-23.16	NA	NA	NA	NA	NA	NA	NA	NA	NA	NA	NA
	RRC22-04	7.8	92.2	6.1	9	100	50	70	20	89	1.03	NA	0.07	0.41	-24.76	NA	NA	NA	NA	NA	NA	NA	NA	NA	NA	NA
	RRC22-05	4.4	95.6	6.3	8	97	56	78	21	98	NA	NA	0.08	0.49	-25.34	NA	NA	NA	NA	NA	NA	NA	NA	NA	NA	NA
	RRC22-06	91.7	8.3	0.2	8	45	20	27	14	31	NA	NA	0.02	0.09	-23.68	NA	NA	NA	NA	NA	NA	NA	NA	NA	NA	NA
	RRC22-07	94.3	5.7	0.1	7	38	14	20	10	21	NA	NA	0.04	0.26	-23.8	NA	NA	NA	NA	NA	NA	NA	NA	NA	NA	NA
	RRC22-08	70.3	29.7	0.4	9	76	20	36	14	45	NA	NA	0.06	0.36	-24	NA	NA	NA	NA	NA	NA	NA	NA	NA	NA	NA
	RRC22-09	46.1	53.9	2.3	11	97	37	62	20	81	0.68	NA	0.07	0.50	-24.98	NA	NA	NA	NA	NA	NA	NA	NA	NA	NA	NA
	RRC22-10	42.8	57.2	1.4	11	93	20	47	16	59	0.51	NA	0.04	0.29	-24.05	NA	NA	NA	NA	NA	NA	NA	NA	NA	NA	NA
	RRC22-11	91.5	8.5	0.2	10	82	24	36	15	44	NA	NA	0.03	0.14	-23.49	NA	NA	NA	NA	NA	NA	NA	NA	NA	NA	NA
	RRC22-12	93.0	7.0	0.2	7	43	22	28	14	31	1.28	NA	0.03	0.09	-22.75	NA	NA	NA	NA	NA	NA	NA	NA	NA	NA	NA
	RRC22-13	63.4	36.6	0.7	8	87	22	20	18	20	0	0	0.02	0.07	-22.5	NA	NA	NA	NA	NA	NA	NA	NA	NA	NA	NA
	RRC22-14	36.2	63.8	1.3	11	66	16	32	13	40	NA	NA	0.04	0.23	-24.49	NA	NA	NA	NA	NA	NA	NA	NA	NA	NA	NA
	RRC22-15	16.2	83.8	3.3	10	84	33	56	20	69	0	0	0.05	0.40	-25.2	NA	NA	NA	NA	NA	NA	NA	NA	NA	NA	NA
	RRC22-16	65.7	34.3	0.6	13	109	31	64	25	93	NA	NA	0.08	0.57	-23.92	NA	NA	NA	NA	NA	NA	NA	NA	NA	NA	NA
	RRC22-17	82.5	17.5	0.3	11	108	16	30	12	35	0	0	0.03	0.11	-22.63	NA	NA	NA	NA	NA	NA	NA	NA	NA	NA	NA
	RRC22-18	91.1	8.9	0.2	9	54	16	26	13	30	NA	NA	0.16	1.08	-25.92	NA	NA	NA	NA	NA	NA	NA	NA	NA	NA	NA
	RRC22-19	90.1	9.9	0.2	9	37	13	24	13	24	0	0	0.03	0.14	-23.2	NA	NA	NA	NA	NA	NA	NA	NA	NA	NA	NA
	RRC22-20	69.5	30.5	0.8	NA	NA	NA	NA	NA	NA	0	0	0.03	0.17	-23.55	NA	NA	NA	NA	NA	NA	NA	NA	NA	NA	NA
	RRC22-21	46.2	53.8	1.6	10	52	16	26	11	29	NA	NA	0.02	0.13	-24.05	NA	NA	NA	NA	NA	NA	NA	NA	NA	NA	NA
	RRC22-22	17.8	82.2	2.6	12	88	16	38	14	48	0	0	0.05	0.26	-24.04	NA	NA	NA	NA	NA	NA	NA	NA	NA	NA	NA
	RRC22-23	85.1	14.9	0.6	NA	NA	NA	NA	NA	NA	NA	NA	0.07	0.51	-24.02	NA	NA	NA	NA	NA	NA	NA	NA	NA	NA	NA
	RRC22-24	57.5	42.5	1.1	NA	NA	NA	NA	NA	NA	0	0	0.03	0.18	-24.54	NA	NA	NA	NA	NA	NA	NA	NA	NA	NA	NA
	RRC22-25	69.9	30.1	0.4	NA	NA	NA	NA	NA	NA	NA	NA	0.02	0.09	-22.99	NA	NA	NA	NA	NA	NA	NA	NA	NA	NA	NA
	RRC22-26	30.0	70.0	2.2	NA	NA	NA	NA	NA	NA	0	0	0.02	0.08	-23.41	NA	NA	NA	NA	NA	NA	NA	NA	NA	NA	NA
	RRC22-27	71.7	28.3	0.4	NA	NA	NA	NA	NA	NA	NA	NA	0.06	0.40	-24.3	NA	NA	NA	NA	NA	NA	NA	NA	NA	NA	NA
	RRC22-28	84.4	15.6	0.3	NA	NA	NA	NA	NA	NA	NA	NA	0.07	0.42	-24.11	NA	NA	NA	NA	NA	NA	NA	NA	NA	NA	NA
	RRC22-29	39.2	57.8	3	NA	NA	NA	NA	NA	NA	0	0	0.02	0.10	-24.36	NA	NA	NA	NA	NA	NA	NA	NA	NA	NA	NA
	RRC22-30	40.2	57.4	2.4	NA	NA	NA	NA	NA	NA	NA	NA	0.02	0.13	-23.28	NA	NA	NA	NA	NA	NA	NA	NA	NA	NA	NA
	RRC22-31	76.6	22.8	0.6	NA	NA	NA	NA	NA	NA	0	0	0.03	0.15	-23.82	NA	NA	NA	NA	NA	NA	NA	NA	NA	NA	NA

Table S1. Summary of the analyses performed on the 2022 flood deposits and the underlying sediments. RRC22: 2022 Rapid Response Cruise; dw: dry weight; FTS: fluorotelomer sulfonate; TN: Total Nitrogen; TOC: Total Organic Carbon; NA: Not Acquired; ND: Not Detected.

PAH compounds	A1	B1	C1	Cesano1	Esino1	Metauro1	Misa1	Musone1	Potenza1
Naphthalene	9.14	0.61	7.15	6.50	0.63	0.78	5.16	0.60	7.91
Acenaphthylene	16.64	17.13	4.02	2.20	5.36	7.53	4.63	5.59	6.97
Acenaphthene	1.94	2.00	3.05	3.11	2.08	2.39	2.49	2.03	2.68
Fluorene	0.64	0.62	0.37	0.40	0.51	0.11	0.50	0.27	0.11
Phenanthrene	7.04	5.49	1.31	2.01	4.03	1.68	3.18	1.14	0.84
Anthracene	2.46	1.72	0.41	0.47	0.90	0.31	0.47	0.38	0.50
Fluoranthene	5.84	6.90	10.53	7.83	3.95	1.41	5.52	1.28	20.15
Pyrene	1.13	0.82	0.35	0.44	1.49	0.40	0.32	0.35	0.36
Benz[*a*]anthracene	0.59	0.26	0.23	0.23	0.57	0.28	0.21	0.27	0.29
Chrysene	1.09	0.36	0.23	0.26	0.58	0.27	0.21	0.28	0.33
Benzo[*b*]fluoranthene	1.65	1.00	0.77	0.60	0.96	0.75	0.58	0.58	0.75
Benzo[*k*]fluoranthene	0.77	0.49	0.45	0.39	0.56	0.49	0.38	0.39	0.48
Benzo[*a*]pyrene	0.79	0.28	0.28	0.12	0.52	0.16	0.18	0.17	0.16
Dibenz[*a.h*]anthracene	0.99	0.89	0.87	0.75	0.87	0.98	0.76	0.76	1.01
Benzo[*ghi*]perylene	0.85	0.65	0.39	0.27	0.51	0.28	0.29	0.25	0.36
Indeno[1,2,3-*cd*]pyrene	0.43	0.17	0.09	0.05	0.17	0.01	0.01	0.04	0.08
Total PAHs	51.97	39.42	30.49	25.63	23.69	17.82	24.89	14.37	42.99
Investigated PAH sources	**A1**	**B1**	**C1**	**Cesano1**	**Esino1**	**Metauro1**	**Misa1**	**Musone1**	**Potenza1**
LMW (2-3 aromatic rings)	37.86	27.58	16.31	14.69	13.51	12.80	16.42	10.01	19.01
HMW (4+ aromatic rings)	14.11	11.84	14.18	10.95	10.18	5.02	8.47	4.36	23.98
LMW/HMW	2.68	2.33	1.15	1.34	1.33	2.55	1.94	2.29	0.79
∑COMB/∑PAHs	0.25	0.28	0.44	0.40	0.39	0.23	0.31	0.25	0.53
Ant/(Ant+Phe)	0.26	0.24	0.24	0.19	0.18	0.16	0.13	0.25	0.38
Flt/(Flt+Pyr)	0.84	0.89	0.97	0.95	0.73	0.78	0.94	0.79	0.98
Phe/Ant	2.87	3.19	3.22	4.28	4.45	5.37	6.80	2.99	1.66
Flt/Pyr	5.18	8.46	30.48	17.83	2.66	3.58	17.16	3.71	55.96
BaA/(BaA+Chr)	0.35	0.42	0.50	0.47	0.49	0.50	0.50	0.49	0.47

Table S2. Concentration (in ng g^{-1} dry weight) of Polycyclic Aromatic Hydrocarbons (PAHs) and their investigated diagnostic ratios in the coastal aliquots of the 2022 flood sediments. LMW: Low Molecular Weight compounds; HMW: High Molecular Weight compounds; COMB: combustion-related compounds; Ant: Anthracene; Phe: Phenanthrene; Flt: Fluoranthene; Pyr: Pyrene; BaA: Benz(*a*)anthracene; Chr: Chrysene.

PAH compounds	A3	B3	C3	Cesano3	Esino3	Metauro3	Misa3	Musone3	Potenza3
Naphthalene	0.81	8.38	0.79	17.11	3.57	7.04	23.78	0.77	0.60
Acenaphthylene	6.09	19.14	8.28	14.76	2.79	6.79	77.57	7.77	3.83
Acenaphthene	2.49	1.99	2.61	3.49	2.52	1.85	4.71	2.47	1.93
Fluorene	0.30	0.58	1.68	1.02	0.21	0.08	0.66	0.11	0.26
Phenanthrene	13.90	11.97	3.04	10.07	3.65	10.29	8.78	3.85	1.59
Anthracene	1.45	2.36	5.88	2.59	6.63	2.91	11.45	0.65	1.64
Fluoranthene	6.33	5.99	1.77	10.83	6.79	7.75	3.99	2.41	1.16
Pyrene	5.16	2.60	0.75	2.17	0.83	1.86	1.77	1.56	0.45
Benz[*a*]anthracene	1.75	0.98	0.47	0.65	0.56	0.44	0.59	0.75	0.32
Chrysene	1.75	1.51	0.60	0.85	0.66	0.95	0.86	0.74	0.34
Benzo[*b*]fluoranthene	2.20	2.64	1.54	1.81	1.67	3.24	2.12	1.11	0.70
Benzo[*k*]fluoranthene	0.99	1.01	0.68	0.66	0.73	1.10	0.81	0.64	0.42
Benzo[*a*]pyrene	1.00	0.93	0.40	0.54	0.71	1.70	0.91	0.32	0.20
Dibenz[*a.h*]anthracene	1.11	1.07	1.16	1.00	1.10	1.05	1.11	0.98	0.76
Benzo[*ghi*]perylene	1.20	1.67	0.89	1.27	1.09	1.58	1.40	0.49	0.33
Indeno[1,2,3-*cd*]pyrene	0.49	0.74	0.36	0.59	0.51	0.91	0.62	0.11	0.08
Total PAHs	47.03	63.55	30.90	69.41	34.01	49.56	141.13	24.76	14.61
Investigated PAH sources	**A3**	**B3**	**C3**	**Cesano3**	**Esino3**	**Metauro3**	**Misa3**	**Musone3**	**Potenza3**
LMW (2-3 aromatic rings)	25.04	44.42	22.29	49.03	19.37	28.97	126.95	15.63	9.86
HMW (4+ aromatic rings)	21.99	19.13	8.61	20.37	14.64	20.59	14.18	9.13	4.75
LMW/HMW	1.14	2.32	2.59	2.41	1.32	1.41	8.96	1.71	2.07
∑COMB/∑PAHs	0.44	0.28	0.24	0.28	0.40	0.39	0.09	0.33	0.27
Ant/(Ant+Phe)	0.09	0.16	0.66	0.20	0.64	0.22	0.57	0.15	0.51
Flt/(Flt+Pyr)	0.55	0.70	0.70	0.83	0.89	0.81	0.69	0.61	0.72
Phe/Ant	9.61	5.07	0.52	3.89	0.55	3.53	0.77	5.88	0.97
Flt/Pyr	1.23	2.31	2.38	4.98	8.18	4.18	2.25	1.54	2.57
BaA/(BaA+Chr)	0.50	0.39	0.44	0.43	0.46	0.31	0.41	0.50	0.48

Table S3. Concentration (in ng g^{-1} dry weight) of Polycyclic Aromatic Hydrocarbons (PAHs) and their investigated diagnostic ratios in the prodelta aliquots of the 2022 flood sediments. LMW: Low Molecular Weight compounds; HMW: High Molecular Weight compounds; COMB: combustion-related compounds; Ant: Anthracene; Phe: Phenanthrene; Flt: Fluoranthene; Pyr: Pyrene; BaA: Benz(*a*)anthracene; Chr: Chrysene.

Transect	Sampling site	Aliquot	PFHxA	PFHpA	PFOA	PFNA	PFDA	PFUnA	PFDoA	PFBS	PFHxS	PFOS	GenX	ADONA	6:2FTS	8:2FTS	PFOSA	*Me*-FOSAA	*Et*-FOSAA
A	Nearshore	*Top*	< MQL	< MQL	< MQL	< MQL	< MQL	< MQL	< MQL	< MQL	< MQL	< MQL	< MQL	< MQL	**10.45**	< MQL	< MQL	< MQL	< MQL
		Bottom	< MQL	< MQL	< MQL	< MQL	< MQL	< MQL	< MQL	< MQL	< MQL	< MQL	< MQL	< MQL	< MQL	< MQL	< MQL	< MQL	< MQL
	Offshore	*Top*	< MQL	< MQL	< MQL	< MQL	< MQL	< MQL	< MQL	< MQL	< MQL	< MQL	< MQL	< MQL	**58.60**	**0.345**	< MQL	< MQL	< MQL
		Bottom	< MQL	< MQL	< MQL	< MQL	< MQL	< MQL	< MQL	< MQL	< MQL	< MQL	< MQL	< MQL	**0.127**	< MQL	< MQL	< MQL	< MQL
Metauro River	Nearshore	*Top*	< MQL	< MQL	< MQL	< MQL	< MQL	< MQL	< MQL	< MQL	< MQL	< MQL	< MQL	< MQL	**85.70**	**0.387**	< MQL	< MQL	< MQL
		Bottom	< MQL	< MQL	< MQL	< MQL	< MQL	< MQL	< MQL	< MQL	< MQL	< MQL	< MQL	< MQL	< MQL	< MQL	< MQL	< MQL	< MQL
	Offshore	*Top*	**0.120**	< MQL	**0.127**	< MQL	< MQL	**0.208**	< MQL	< MQL	< MQL	< MQL	< MQL	< MQL	**65.34**	**0.254**	< MQL	< MQL	< MQL
		Bottom	< MQL	< MQL	< MQL	< MQL	< MQL	< MQL	< MQL	< MQL	< MQL	< MQL	< MQL	< MQL	**0.286**	< MQL	< MQL	< MQL	< MQL
B	Nearshore	*Top*	< MQL	< MQL	< MQL	< MQL	< MQL	< MQL	< MQL	< MQL	< MQL	< MQL	< MQL	< MQL	**86.10**	**0.439**	< MQL	< MQL	< MQL
		Bottom	< MQL	< MQL	< MQL	< MQL	< MQL	< MQL	< MQL	< MQL	< MQL	< MQL	< MQL	< MQL	< MQL	< MQL	< MQL	< MQL	< MQL
	Offshore	*Top*	< MQL	< MQL	< MQL	< MQL	< MQL	< MQL	< MQL	< MQL	< MQL	< MQL	< MQL	< MQL	**38.60**	**0.210**	< MQL	< MQL	< MQL
		Bottom	< MQL	< MQL	< MQL	< MQL	< MQL	< MQL	< MQL	< MQL	< MQL	< MQL	< MQL	< MQL	**0.188**	< MQL	< MQL	< MQL	< MQL
Cesano River	Nearshore	*Top*	< MQL	< MQL	< MQL	< MQL	< MQL	< MQL	< MQL	< MQL	< MQL	< MQL	< MQL	< MQL	**0.790**	< MQL	< MQL	< MQL	< MQL
		Bottom	< MQL	< MQL	< MQL	< MQL	< MQL	< MQL	< MQL	< MQL	< MQL	< MQL	< MQL	< MQL	**0.355**	< MQL	< MQL	< MQL	< MQL
	Offshore	*Top*	< MQL	< MQL	< MQL	< MQL	< MQL	< MQL	< MQL	< MQL	< MQL	< MQL	< MQL	< MQL	**0.880**	< MQL	< MQL	< MQL	< MQL
		Bottom	< MQL	< MQL	< MQL	< MQL	< MQL	< MQL	< MQL	< MQL	< MQL	< MQL	< MQL	< MQL	**0.142**	< MQL	< MQL	< MQL	< MQL
Misa River	Nearshore	*Top*	< MQL	< MQL	< MQL	< MQL	< MQL	< MQL	< MQL	< MQL	< MQL	< MQL	< MQL	< MQL	**45.18**	**0.251**	< MQL	< MQL	< MQL
		Bottom	< MQL	< MQL	< MQL	< MQL	< MQL	< MQL	< MQL	< MQL	< MQL	< MQL	< MQL	< MQL	< MQL	< MQL	< MQL	< MQL	< MQL
	Offshore	*Top*	< MQL	< MQL	< MQL	< MQL	< MQL	< MQL	< MQL	< MQL	< MQL	< MQL	< MQL	< MQL	**0.625**	< MQL	< MQL	< MQL	< MQL
		Bottom	< MQL	< MQL	< MQL	< MQL	< MQL	< MQL	< MQL	< MQL	< MQL	< MQL	< MQL	< MQL	< MQL	< MQL	< MQL	< MQL	< MQL
C	Nearshore	*Top*	< MQL	< MQL	< MQL	< MQL	< MQL	< MQL	< MQL	< MQL	< MQL	< MQL	< MQL	< MQL	**0.412**	< MQL	< MQL	< MQL	< MQL
		Bottom	< MQL	< MQL	< MQL	< MQL	< MQL	< MQL	< MQL	< MQL	< MQL	< MQL	< MQL	< MQL	< MQL	< MQL	< MQL	< MQL	< MQL
	Offshore	*Top*	< MQL	< MQL	< MQL	< MQL	< MQL	< MQL	< MQL	< MQL	< MQL	< MQL	< MQL	< MQL	**0.341**	< MQL	< MQL	< MQL	< MQL
		Bottom	< MQL	< MQL	< MQL	< MQL	< MQL	< MQL	< MQL	< MQL	< MQL	< MQL	< MQL	< MQL	< MQL	< MQL	< MQL	< MQL	< MQL
Esino River	Nearshore	*Top*	< MQL	< MQL	< MQL	< MQL	< MQL	< MQL	< MQL	< MQL	< MQL	< MQL	< MQL	< MQL	**0.500**	< MQL	< MQL	< MQL	< MQL
		Bottom	< MQL	< MQL	< MQL	< MQL	< MQL	< MQL	< MQL	< MQL	< MQL	< MQL	< MQL	< MQL	< MQL	< MQL	< MQL	< MQL	< MQL
	Offshore	*Top*	< MQL	< MQL	< MQL	< MQL	< MQL	< MQL	< MQL	< MQL	< MQL	**0.052**	< MQL	< MQL	**0.203**	< MQL	< MQL	< MQL	< MQL
		Bottom	< MQL	< MQL	< MQL	< MQL	< MQL	< MQL	< MQL	< MQL	< MQL	< MQL	< MQL	< MQL	< MQL	< MQL	< MQL	< MQL	< MQL
Musone River	Nearshore	*Top*	< MQL	< MQL	< MQL	< MQL	< MQL	< MQL	< MQL	< MQL	< MQL	< MQL	< MQL	< MQL	< MQL	< MQL	< MQL	< MQL	< MQL
		Bottom	< MQL	< MQL	< MQL	< MQL	< MQL	< MQL	< MQL	< MQL	< MQL	< MQL	< MQL	< MQL	< MQL	< MQL	< MQL	< MQL	< MQL
	Offshore	*Top*	< MQL	< MQL	< MQL	< MQL	< MQL	< MQL	< MQL	< MQL	< MQL	< MQL	< MQL	< MQL	< MQL	< MQL	< MQL	< MQL	< MQL
		Bottom	< MQL	< MQL	< MQL	< MQL	< MQL	< MQL	< MQL	< MQL	< MQL	< MQL	< MQL	< MQL	< MQL	< MQL	< MQL	< MQL	< MQL
Potenza River	Nearshore	*Top*	< MQL	< MQL	< MQL	< MQL	< MQL	< MQL	< MQL	< MQL	< MQL	< MQL	< MQL	< MQL	< MQL	< MQL	< MQL	< MQL	< MQL
		Bottom	< MQL	< MQL	< MQL	< MQL	< MQL	< MQL	< MQL	< MQL	< MQL	< MQL	< MQL	< MQL	< MQL	< MQL	< MQL	< MQL	< MQL
	Offshore	*Top*	< MQL	< MQL	< MQL	< MQL	< MQL	< MQL	< MQL	< MQL	< MQL	< MQL	< MQL	< MQL	< MQL	< MQL	< MQL	< MQL	< MQL
		Bottom	< MQL	< MQL	< MQL	< MQL	< MQL	< MQL	< MQL	< MQL	< MQL	< MQL	< MQL	< MQL	< MQL	< MQL	< MQL	< MQL	< MQL
MQLs (ng abs)			0,456	0,414	0,121	0,060	0,290	0,629	0,365	3,861	1,074	0,624	2,276	0,570	1,100	0,968	0,007	0,349	0,910

Table S4. Concentrations (in ng g^{-1} dry weight) of Poly- and Perfluorinated alkyl substances (PFASs) in the sediment aliquots (*Top* and *Bottom* refer to the 2022 flood sediments and those underlying the flood event, respectively) of the nine coast-to-offshore studied transects. MQL: Method Quantification Limit. PFHxA: Perfluorohexanoic acid; PFHpA: Perfluoroheptanoic acid; PFOA: Perfluorooctanoic acid; PFNA: Perfluorononanoic acid; PFDA: Perfluorodecanoic acid; PFUnA: Perfluoroundecanoic acid; PFDoA: Perfluorododecanoic acid; PFBS: Perfluorobutanesulfonic acid; PFHxS: Perfluorohexanesulfonic acid; PFOS: Perfluorooctanesulfonic acid; GenX: Hexafluoropropylene oxide dimer acid (HFPO-DA); ADONA: 3H-perfluoro-3-[(3-methoxy-propoxy)propanoic acid]; 6:2 FTS: 6:2-fluorotelomersulfonate; 8:2 FTS: 8:2-fluorotelomersulfonate; PFOSA: Perfluorooctanesulfonamide; *Me*-FOSAA: Methylperfluorooctanesulfonamidoacetic acid; *Et*-FOSAA: Ethylperfluorooctanesulfonamidoacetic acid.

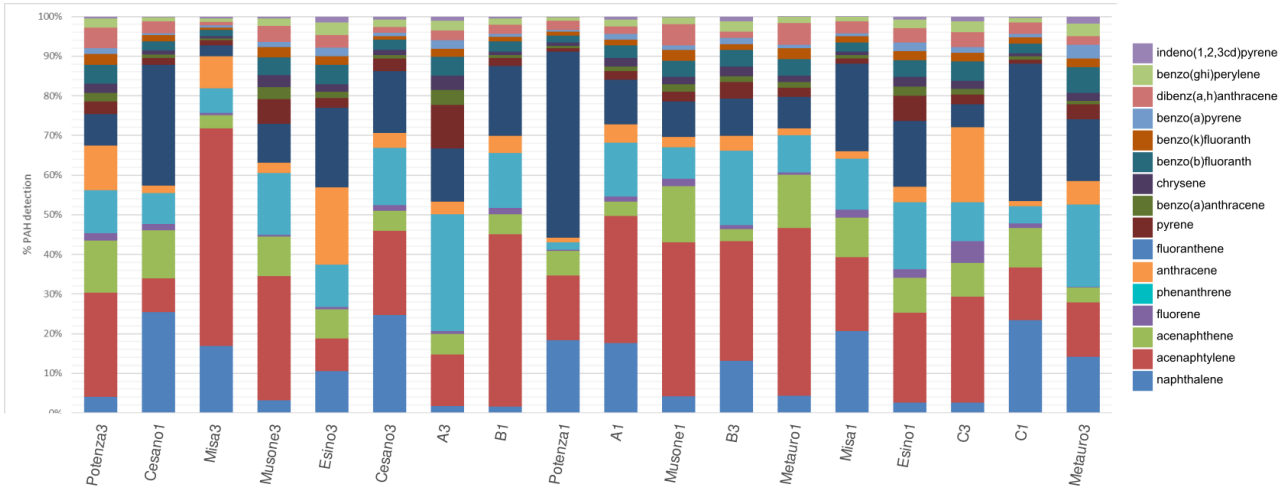

Figure S1. Distribution patterns of Polycyclic Aromatic Hydrocarbons (PAHs) in the analyzed sediments.

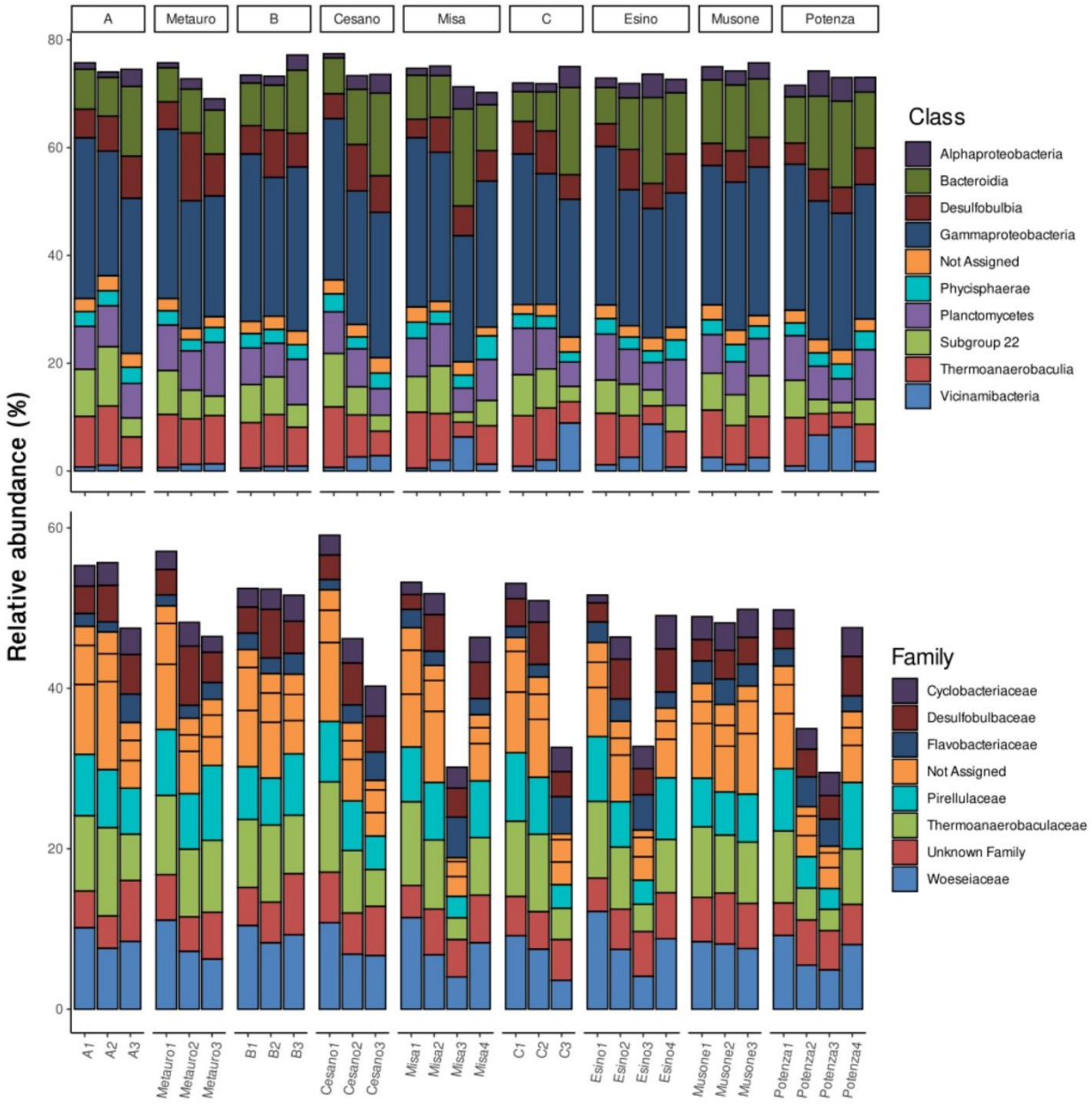

Figure S2. Barplot showing the prokaryotic community composition (as relative abundance) at the class and family levels, separated according to transects. Only the ten most abundant taxa were showed.

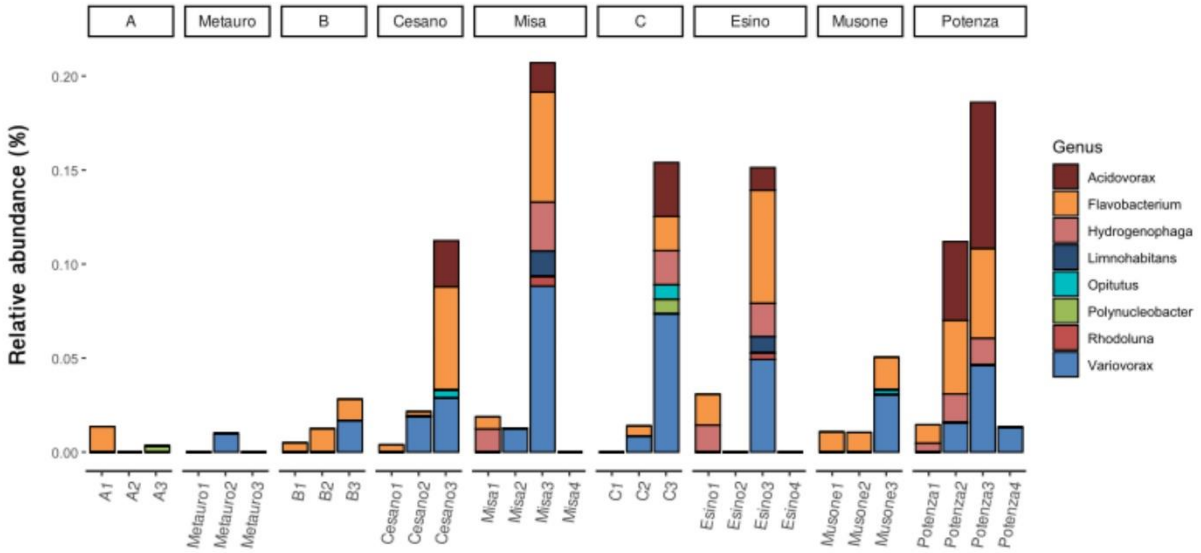

Figure S3. Barplot showing the dominant bacterial genera (as relative abundance), separated according to transects.

REFERENCES

Amorosi, A., Sammartino, I., Dinelli, E., Campo, B., Guercia, T., Trincardi, F., and Pellegrini, C.: Provenance and sediment dispersal in the Po-Adriatic source-to-sink system unraveled by bulk-sediment geochemistry and its linkage to catchment geology, Earth-Sci. Rev., 234, 104202, 2022. https://doi.org/10.1016/j.earscirev.2022.104202

Blott, S. J. and Pye, K.: GRADISTAT: a grain size distribution and statistics package for the analysis of unconsolidated sediments, Earth Surf. Process. Landforms, 26, 1237–1248, 2001. https://doi.org/10.1002/esp.261

Bressan, L., Valentini, A., Paccagnella, T., Montani, A., Marsigli, C., and Tesini, M. S.: Sensitivity of sea-level forecasting to the horizontal resolution and sea surface forcing for different configurations of an oceanographic model of the Adriatic Sea, Adv. Sci. Res., 14, 77–84, 2017 https://doi.org/10.5194/asr-14-77-2017

Callahan, B. J., McMurdie, P. J., Rosen, M. J., Han, A. W., Johnson, A. J. A., and Holmes, S. P.: DADA2: High-resolution sample inference from Illumina amplicon data, Nat. Methods, 13, 581–583, 2016. https://doi.org/10.1038/nmeth.3869

Davolio, S., Henin, R., Stocchi, P., and Buzzi, A.: Bora wind and heavy persistent precipitation: atmospheric water balance and role of air–sea fluxes over the Adriatic Sea, Q. J. R. Meteorol. Soc., 143, 1165–1177, 2017, https://doi.org/10.1002/qj.3004

Dinelli, E., Lucchini, F., Mordenti, A., and Paganelli, L.: Geochemistry of Oligocene–Miocene sandstones of the northern Apennines (Italy) and evolution of chemical features in relation to provenance changes, Sediment. Geol, 127, 193–207, 1999. https://doi.org/10.1016/S0037-0738(99)00049-4

Franzini, M., Leoni, L., and Saitta, M.: A simple method to evaluate the matrix effects in X-Ray fluorescence analysis, X-Ray Spectrom., 1, 151–154, 1972. https://doi.org/10.1002/xrs.1300010406

Franzini, M., Leoni, L., and Saitta, M.: Revisione di una metodologia analitica per fluorescenza X, basata sulla correzione completa degli effetti di matrice, Rend. Soc. Ital. Mineral. Petrol., 31, 365–378, 1975.

Frapiccini, E., De Marco, R., Grilli, F., Marini, M., Annibaldi, A., Prezioso, E., Tramontana, M., and Spagnoli, F.: Anthropogenic contribution, transport, and accumulation of polycyclic aromatic hydrocarbons in sediments of the continental shelf and slope in the Mediterranean Sea, Chemosphere, 352, 141285, 2024. https://doi.org/10.1016/j.chemosphere.2024.141285

Govindaraju, K.: 1989 compilation of working values and sample description for 272 geostandards, Geostandards Newsletter, 13, 1–113, 1989. https://doi.org/10.1111/j.1751-908X.1989.tb00476.x

Leoni, L. and Saitta, M.: Determination of yttrium and niobium on standard silicate rocks by X-ray fluorescence analyses, X-Ray Spectrom., 5, 29–30, 1976. https://doi.org/10.1002/xrs.1300050107

Martin, M.: Cutadapt removes adapter sequences from high-throughput sequencing reads, EMBnet J., 17, 10–12, 2011. https://doi.org/10.14806/ej.17.1.200

Massaccesi, N., Basili, M., Coci, M., Cassin, D., Zonta, R., Manini, E., and Quero, G. M.: Benthic prokaryotic diversity in Po River Delta lagoons (North Adriatic Sea) is shaped by riverine freshwater inputs, Estuar. Coast. Shelf Sci., 109348, 2025. https://doi.org/10.1016/j.ecss.2025.109348

McMurdie, P. J. and Holmes, S.: phyloseq: an R package for reproducible interactive analysis and graphics of microbiome census data, PLoS ONE, 8, e61217, 2013. https://doi.org/10.1371/journal.pone.0061217

Oksanen, J., Simpson, G. L., Blanchet, F. G., Kindt, R., Legendre, P., Minchin, P. R., O'Hara, R. B., Solymos, P., Stevens, M. H. H., Szoecs, E., and Wagner, H.: vegan: Community Ecology Package, R package version 2.6-8, CRAN [code], 2025. https://cran.r-project.org/package=vegan

Parada, A. E., Needham, D. M., and Fuhrman, J. A.: Every base matters: assessing small subunit rRNA primers for marine microbiomes with mock communities, time series and global field samples, Environ. Microbiol., 18, 1403–1414, 2016. https://doi.org/10.1111/1462-2920.13023

Pellegrini, C., Tesi, T., Schieber, J., Bohacs, K. M., Rovere, M., Asioli, A., and Trincardi, F.: Fate of terrigenous organic carbon in muddy clinothems on continental shelves revealed by stratal geometries: Insight from the Adriatic sedimentary archive, Global Planet. Change, 203, 103539, 2021. https://doi.org/10.1016/j.gloplacha.2021.103539

Pellegrini, C., Sammartino, I., Schieber, J., Tesi, T., Paladini de Mendoza, F., Rossi, V., and Amorosi, A.: On depositional processes governing along-strike facies variations of fine-grained deposits: Unlocking the Little Ice Age subaqueous clinothems on the Adriatic shelf, Sedimentology, 71, 941–973, 2024. https://doi.org/10.1111/sed.13162

Pizzini, S., Giubilato, E., Morabito, E., Barbaro, E., Bonetto, A., Calgaro, L., and Marcomini, A.: Contaminants of emerging concern in water and sediment of the Venice Lagoon, Italy, Environ. Res., 249, 118401, 2024. https://doi.org/10.1016/j.envres.2024.118401

Quast, C., Pruesse, E., Yilmaz, P., Gerken, J., Schweer, T., Yarza, P., Peplies, J., and Glöckner, F. O.: The SILVA ribosomal RNA gene database project: improved data processing and web-based tools, Nucleic Acids Res., 41, D590–D596, 2013. https://doi.org/10.1093/nar/gks1219

Ravaioli, M., Bergami, C., Riminucci, F., Langone, L., Cardin, V., Di Sarra, A., and Crise, A.: The RITMARE Italian Fixed-Point Observatory Network (IFON) for marine environmental monitoring: a case study, J. Oper. Oceanogr., 9, s202–s214, 2016. https://doi.org/10.1080/1755876X.2015.1115631

Schieber, J.: SEM observations on ion-milled samples of Devonian black shales from Indiana and New York: the petrographic context of multiple pore types, 2013. https://doi.org/10.1306/13391711M1023589

Schimmelmann, A., Riese, D. J., and Schieber, J.: Fast and economical sampling and resin-embedding technique for small cores of unconsolidated, fine-grained sediment, in: Proceedings of the 2015 Pacific Climate (PACLIM) Workshop, Asilomar Conference Grounds, Pacific Grove, CA, USA, 8–11, 2015.

Segata, N., Izard, J., Waldron, L., Gevers, D., Miropolsky, L., Garrett, W. S., and Huttenhower, C.: Metagenomic biomarker discovery and explanation, Genome Biol., 12, R60, 2011. https://doi.org/10.1186/gb-2011-12-6-r60

Tesi, T., Miserocchi, S., Goñi, M. E. A., Langone, L., Boldrin, A., and Turchetto, M.: Organic matter origin and distribution in suspended particulate materials and surficial sediments from the western Adriatic Sea (Italy), Estuar. Coast. Shelf Sci., 73, 431–446, 2007. https://doi.org/10.1016/j.ecss.2007.02.008

Tesi, T., Langone, L., Giani, M., Ravaioli, M., and Miserocchi, S.: Source, diagenesis, and fluxes of particulate organic carbon along the western Adriatic Sea (Mediterranean Sea), Mar. Geol., 337, 156–170, 2013. https://doi.org/10.1016/j.margeo.2013.03.001

Warner, J. C., Armstrong, B., He, R., and Zambon, J. B.: Development of a coupled ocean–atmosphere–wave–sediment transport (COAWST) modeling system, Ocean Model., 35, 230–244, 2010 https://doi.org/10.1016/j.ocemod.2010.07.010

Wentworth, C. K.: A scale of grade and class terms for clastic sediments, J. Geol., 30, 377–392, 1922. https://doi.org/10.1086/622910